Electronic Supplementary Material (ESI) for Chemical Science.

Electronic Supporting Information (ESI) for:

Flavanthrene derivatives as photostable and efficient singlet exciton fission materials

Xian Fei,‡[a] San Zhang,‡[b] Dong Zhai,‡[c] Zhiwei Wang,[b] Jin-Liang Lin,[a] Qi Xiao,[a] Chun-Lin Sun,[a] Weiqiao Deng,*[c] Chunfeng Zhang,*[b] Wenping Hu,*[d] Hao-Li Zhang*[ad]

Table of Contents

1. Materials and Methods……………………………………………………………………S2

2. Experimental section

GIWAXS Measurements…………………………………………………………S4

Stability characterization……………………………………………………….....S4

Steady-state spectra………………………………………………………………..S5

Phosphorescence spectra……………………………………………………………S6

FsTA absorption in dilute solution………………………………………………..S6

Excitation fluence dependence…………………………..............................S8

Near-infrared region fs-TA…………………………..................................S8

Temperature dependence experience……………………………………………...S9

Ns-TA transient spectroscopy………………………………………………………S11

Triplet sensitization…………………………………………………………………..S12

Thermal effect………………………………………………………………………...S14

Triplet yield calculation………………………………………………………………S14

Quantum Chemical calculation…………………………………………………….S15

Crystal data…………………………………………………………………………...S17

3. Reference……………………………………………………………………………S17

1. Materials and methods

Film preparation and Characterization

The TIPS-Fla film was prepared by a self-made tube furnace. The sample was placed in the high-temperature area of the tube furnace, the temperature was set to 265 °C, the quartz was placed in the low-temperature area (room temperature), and the sample was deposited at 5×10^{-5} Pa for one hour. The EH-Fla films were prepared by spin coating. 15 mg EH-Fla was dissolved in chloroform and spin-coated on quartz at 1500 rpm. The crystallinity of the film was further improved by thermal annealing at 120 °C for 10 minutes.

Steady-state spectroscopy characterization

The steady-state absorption spectrum is measured by a T6 UV-Vis spectrometer (Purkinje General, China). Photoluminescence spectrum was obtained by FLS920 (Edinburgh, UK). Phosphorescence spectra of EH-Fla and TIPS-Fla were done on PerkinElmer (American) in argon-saturated Methyl-tetrahydrofuran containing MeI (10 mM) at 77 K.

Femtosecond transient absorption spectroscopy (fs-TA)

A Coherent Chameleon oscillator seeded a Ti/sapphire regenerative amplifier (Coherent Legend Elite) to produce pulses of about 100 fs duration at a repetition rate of 1 kHz and a wavelength centred at 800 nm. The 400 nm pump pulse was generated from a Light Conversion OPerA-Solo optical parametric amplifier (285-2600 nm). The white probe pulse was produced by focusing a small portion of the 800 nm beam on the sapphire plate for measurements in the visible region. All characterization was performed at room temperature unless otherwise specified.

Global Target Analysis (GTA)

Glotaran was used to perform a **GTA** in this study, an approach that starts with a simple model with a defined number of components and a set of starting values for rate constants that describe the kinetic connections between the components. The entire TA dataset was fitted by generating a time-dependent population evolution of spectral intensities from a set of first-order differential equations. The parameters are then optimized by re-tuning the starting values based on the resulting model. The quality of the fit can be judged by the fitted spectral and time traces and the residual matrix. Any residual structure in the singular vector shows a potential mismatch and the need for another component in the proposed model. After examining and accepting the fitted model, the program generates kinetic trajectories, population evolution, and spectra for each component. GTA was used to separate overlapping features and generate population profiles versus time for each component.

Before performing global fitting, we performed singular value decomposition (SVD) on the experimental data, and the results of SVD showed that there are three states in EH-Fla. For EH-Fla, the branched model does no give a good fit, and the best fit of EH-Fla is obtained using a 3-state sequential model.

For TIPS-Fla, the SVD results show that there are two states. We observed that with the decay of the ESA signal at 700 nm, a new ESA signal was produced at 540 nm, showing a clear sequential process. The best fit to the fs-TA of TIPS-Fla is obtained using a 2-state sequential model.

Nanosecond transient absorption spectroscopy (ns-TA)

Nanosecond transient absorption spectroscopy was used to further characterize the dynamics of long-lived species. The pump pulse was generated by a frequency-tripled sub-nanosecond laser (Picolo AOT MOPA, InnoLas) at 355 nm (duration ~0.8 ns). The probe beam was a broadband chirp-corrected supercontinuum light source generated by focusing a small portion of the femtosecond laser beam onto a 3 mm-thick sapphire plate for the visible range. The laser was synchronized to the probe pulse with a desired delay by an electronic delay generator (SRS DG645, Stanford Research System).

2. Experimental section

GIWAXS measurements

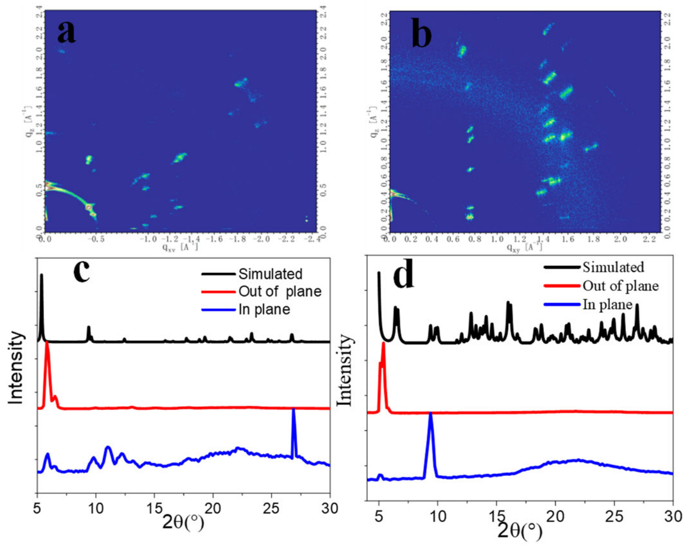

Figure S1. Comparison of the in-plane and out-of-plane line cuts from GIWAXS with simulated powder patterns (black lines) of EH-Fla (a, c) and TIPS-Fla (b, d).

Stability characterization

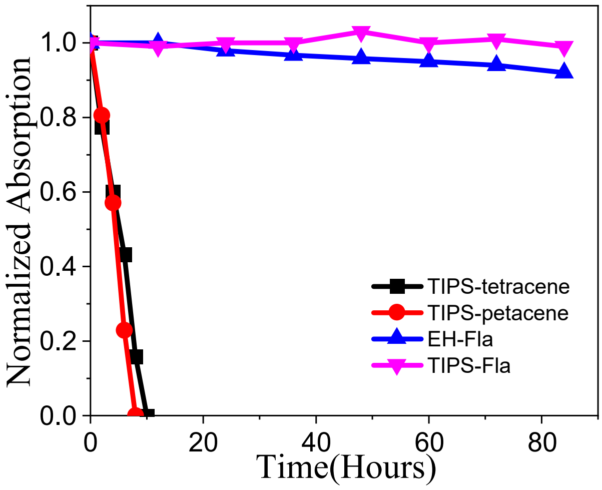

Figure S2. Normalized intensity of the absorbance at the maxium absorption wavelength (λ_{max})of the steady-state absorbance spectra of flavanhrene derivatives, TIPS-tetracene and TIPS-pentacene in toluene solutions under 365 nm 18 W UV lamp irradiation.

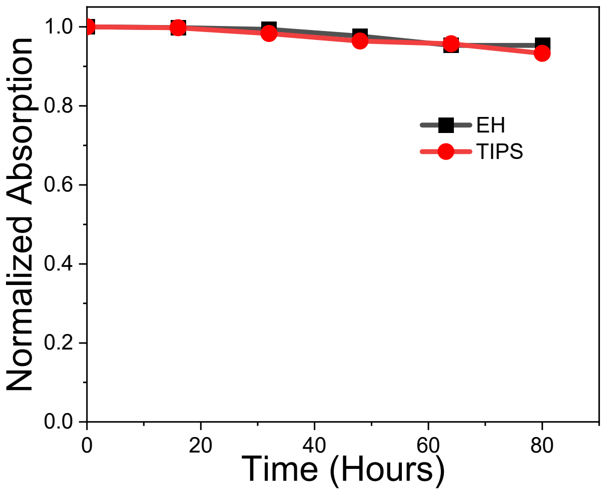

Figure S3. Normalized intensity of the λ_{max} of the steady-state absorption spectra of EH-Fla and TIPS-Fla thin films under 365 nm 18 W UV lamp irradiation.

Steady-state spectra

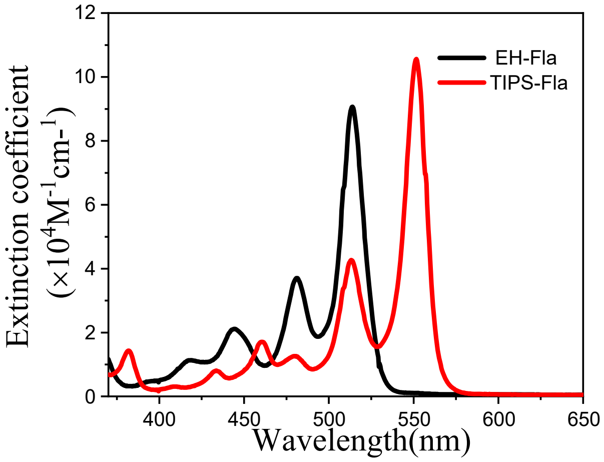

Figure S4. The steady-state absorption spectra of EH-Fla and TIPS-Fla in dichloromethane.

Phosphorescence spectra

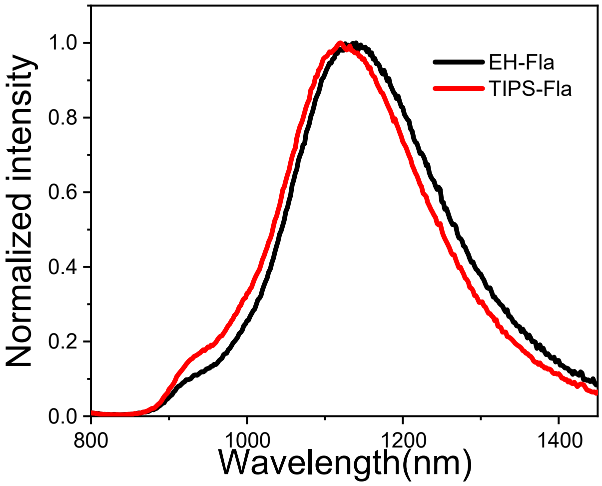

Figure S5. Phosphorescence spectra of EH-Fla and TIPS-Fla in argon-saturated Methyl-tetrahydrofuran containing MeI (10 mM) at 77 K.

Fs-TA absorption in dilute solutions

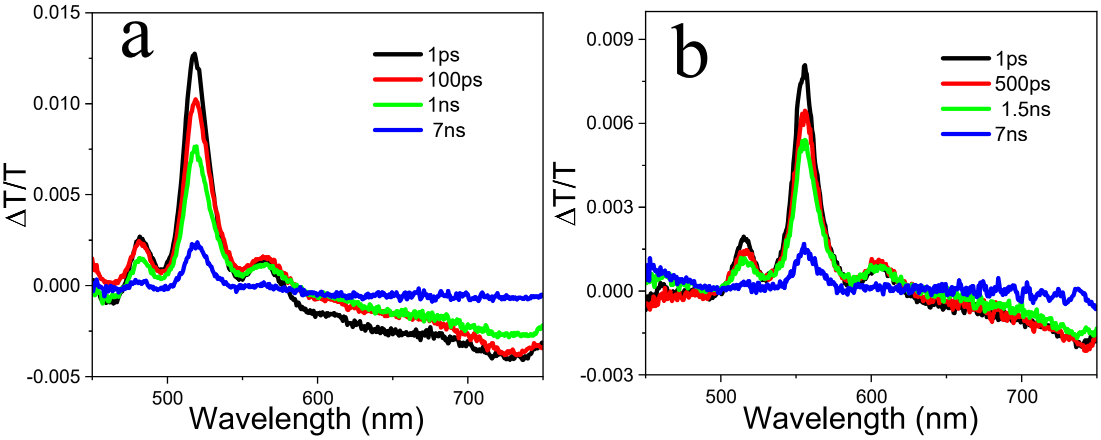

Figure S6. Fs-TA spectra of EH-Fla (a) and TIPS-Fla (b) excited at 400 nm in dilute dichloromethane solutions.

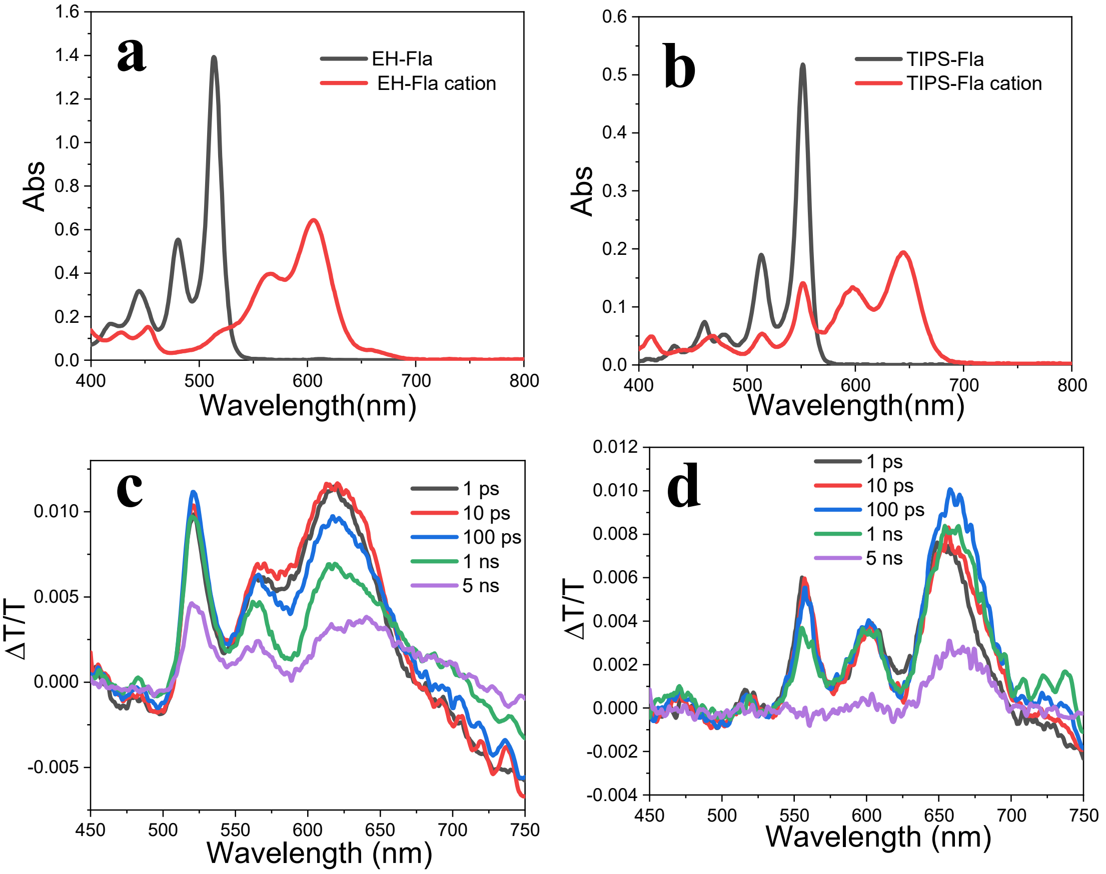

Figure S7. a) The absorption spectra of EH-Fla in dichloromethane and EH-Fla cation produced by adding hydrochloric acid. b) The absorption spectra of TIPS-Fla in dichloromethane and TIPS-Fla cation produced by adding hydrochloric acid. Figure c, d. fs-TA of EH-Fla cations (c) and TIPS-Fla cations (d) excited at 400 nm in dichloromethane.

Figure S7b shows that the absorption of the TIPS-Fla cation is reduced by 500–575 nm compared with TIPS-Fla, with a new strong absorption feature around 575–675 nm. Under photoexcitation of this sample, these features appear as a GSB at 575–675 nm, especially at about 650 nm. Therefore, if a CT state exists, when exciting the thin film sample, a photo induced absorption (PIA) signal should be observed around 650 nm. However, our fs-TA spectra do not show the signal of PIA around 650nm. Therefore, the fs-TA spectra can rule out the direct involvement of the real CT state.

Excitation fluence dependent kinetic decay curves

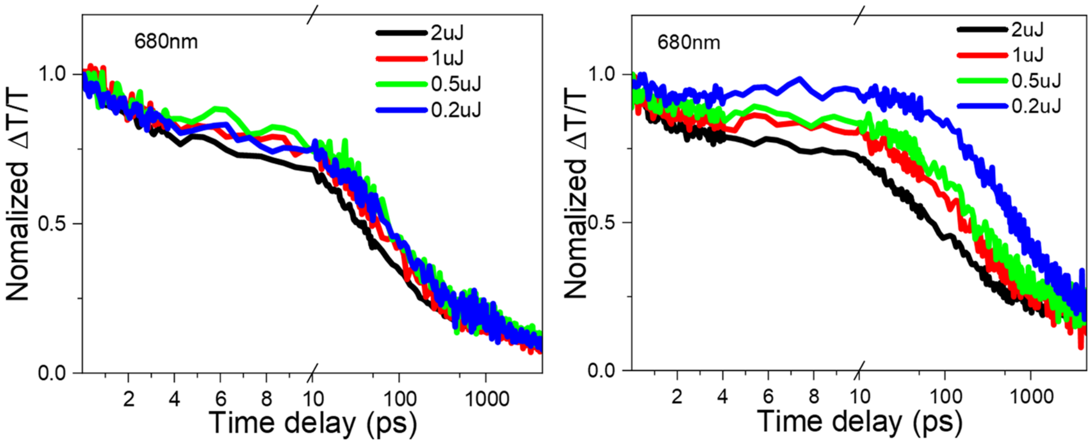

Figure S8. Normalized kinetic decay curves at 680 nm at different excitation fluences of EH-Fla (a) and TIPS-Fla (b) in the film.

Near-infrared region fs-TA spectra

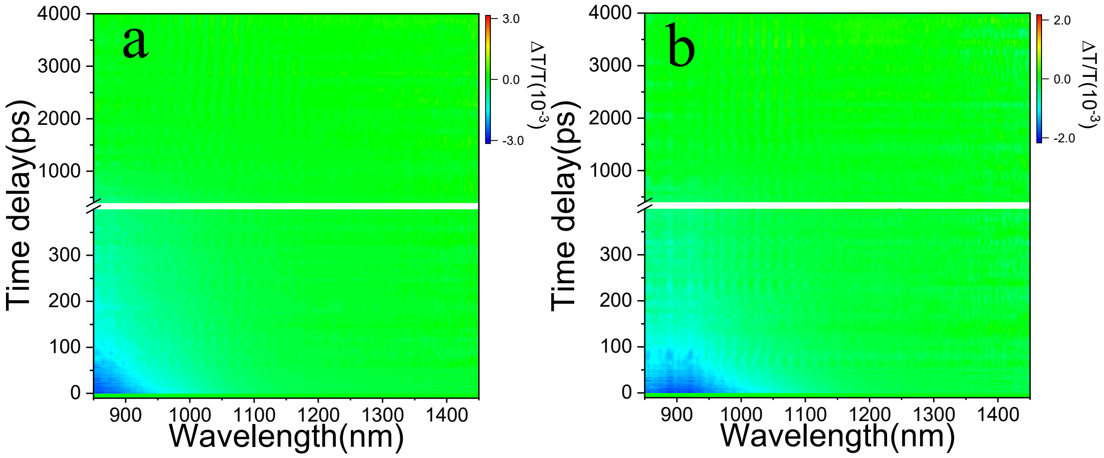

Figure S9. Near-infrared region fs-TA spectra of EH-Fla (a) and TIPS-Fla (b).

Temperature dependence experiments

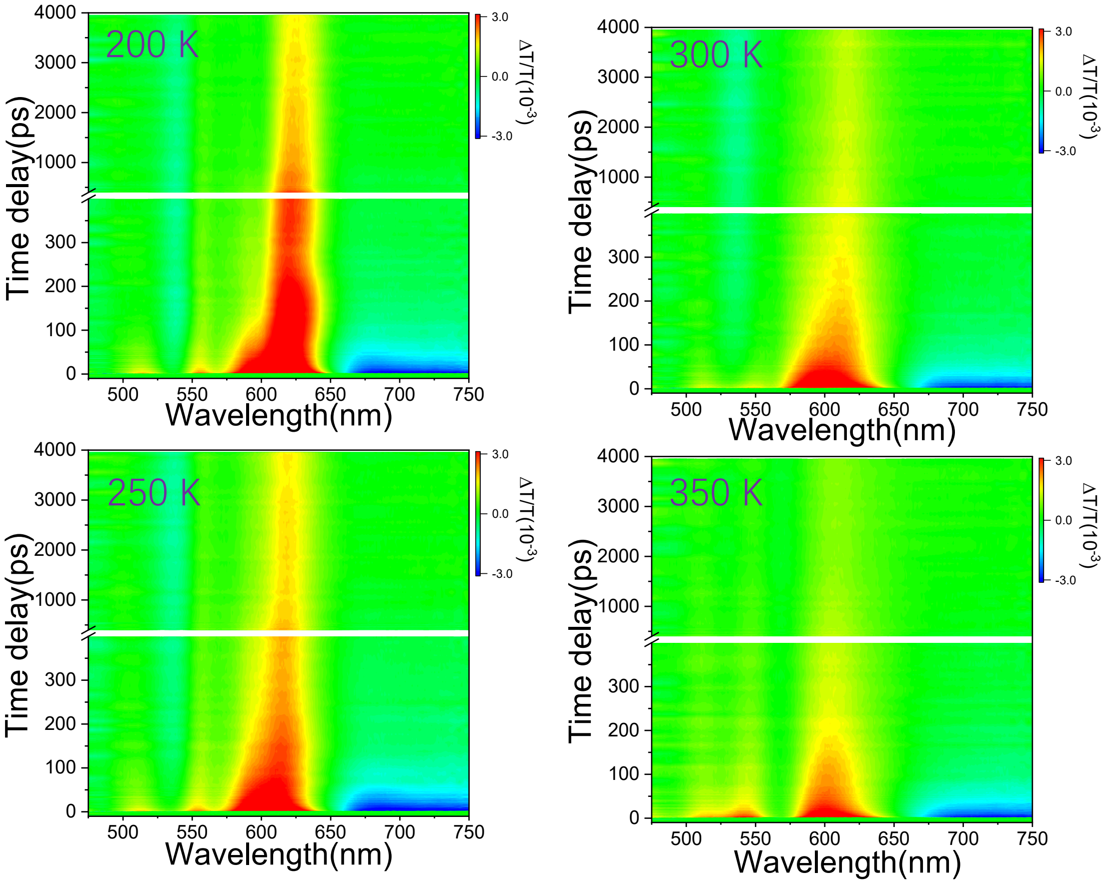

Figure S10. The fs-TA spectra of TIPS-Fla at different temperatures.

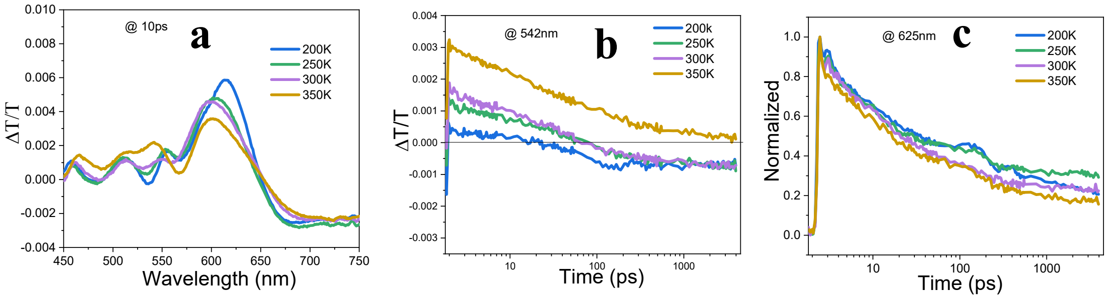

Figure S11. a) The fs-TA spectra of TIPS-Fla at 10 ps at different temperatures. b) The kinetic curves of TIPS-Fla at 542 nm at different temperatures. c) The kinetic curves of TIPS-Fla at 625 nm at different temperatures.

The experimental results of temperature dependent fs-TA spectra are shown in Figure S10 and S11. With the increase of temperature, the peak is gradually red-shifted and its intensity weakened, accompanied by an increase in the intensity of the peak between 450 nm and 550 nm. Further, increase the temperature to 350 K, no triplet was observed.

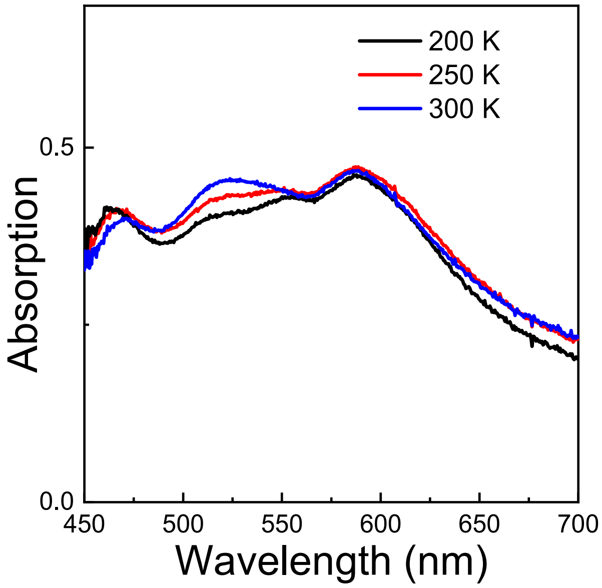

Figure S12. Absorption spectra of TIPS-Fla at different temperatures.

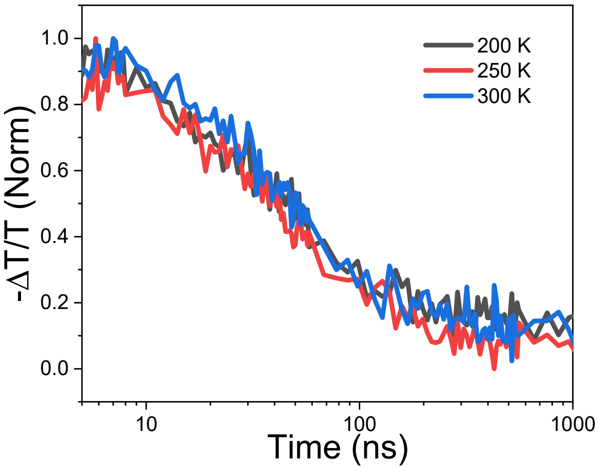

Figure S13. The kinetic curves of TIPS-Fla at 536 nm at different temperatures.

The results show that the kinetic curves at different temperatures are not significantly different, indicating that the kinetic process at nanosecond to microsecond time scales is temperature-independent.

ns-TA spectra

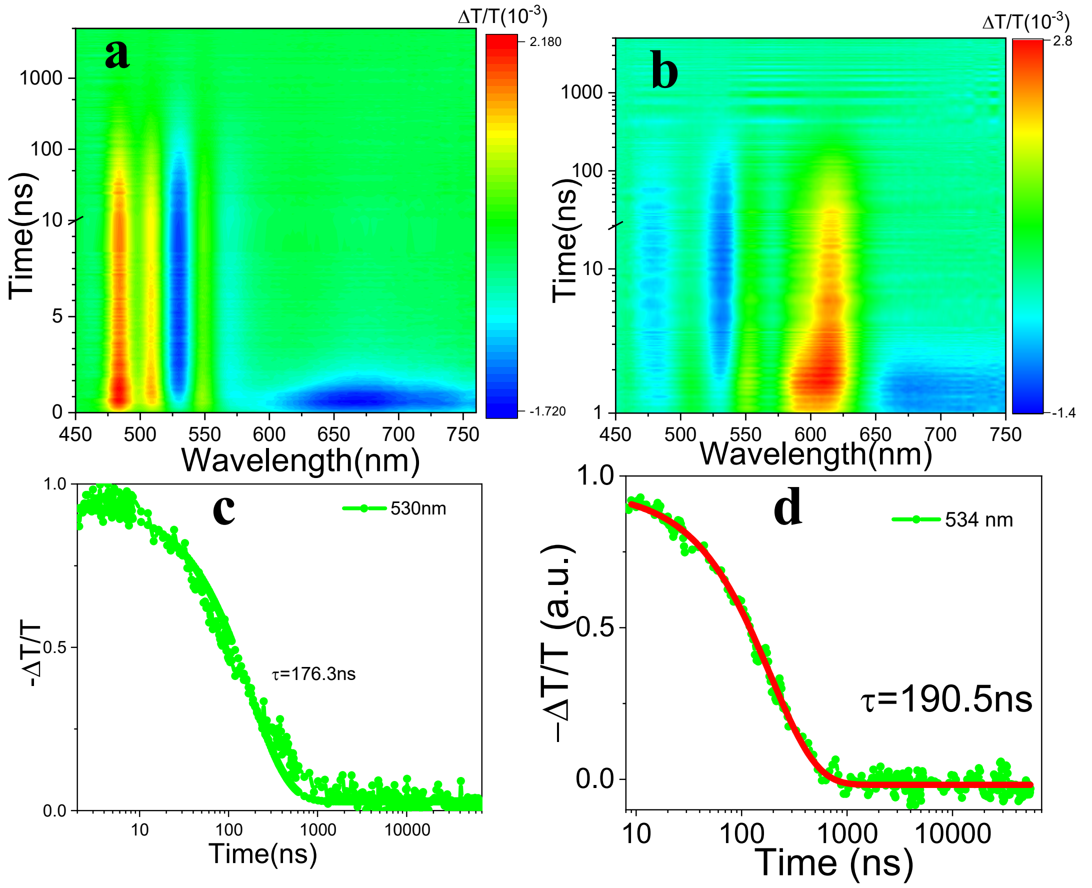

Figure S14. Raw ns-TA spectra of EH-Fla (a) and TIPS-Fla (b) films excited at 365 nm, and the corresponding decay kinetics of EH-Fla at 530 nm and TIPS-Fla at 534 nm.

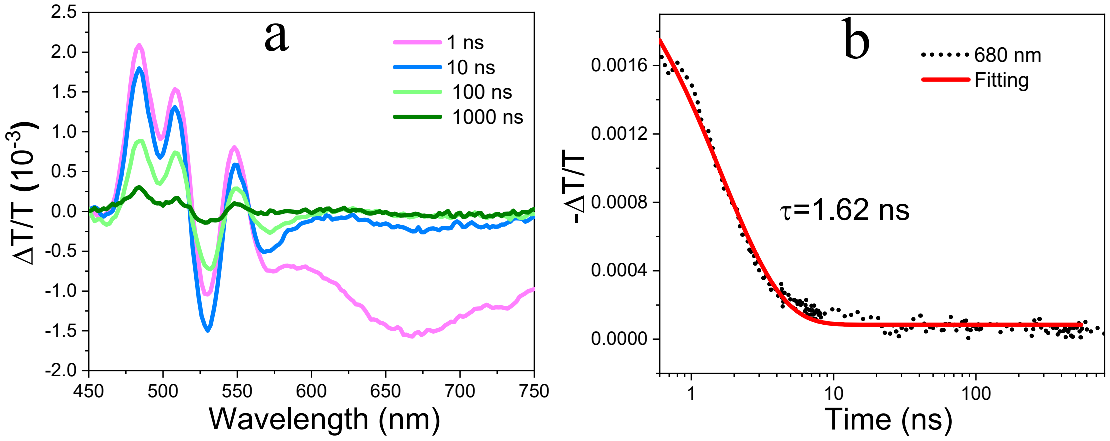

Figure S15. The ns-TA spectra of EH-Fla at different delay times and decay kinetics of at 680 nm.

The red/NIR photo induced absorption (PIA) in ns-TA spectra disappears completely in about 13ns. Fitting to the curve indicates a lifetime of 1.62 ns for this signal. There is no signal in red/NIR region on longer time scales, therefore we truncated the comparison in Figure S17 at 600nm (EH-Fla) or 650nm (TIPS-Fla) for clarity.

Triplet sensitization

To obtain the triplet spectra of EH-Fla and TIPS-Fla, the sample and sensitizer palladium octabutoxyphthalocyanine ($PdPc(OBu)_8$) were dissolved in chloroform and then spin-coated on quartz at 1500 rpm. The sensitized films were excited at 720 nm, at which wavelength only the sensitizer was excited. $PdPc(OBu)_8$ was selected as the triplet sensitizer for its rapid and quantitative intersystem crossing property. The triplet energy of $PdPc(OBu)_8$ is 1.24 eV,[1] which can transfer triplet energy to EH-Fla and TIPS-Fla. We measured the fs-TA spectra of $PdPc(OBu)_8$-doped flavanthren films following selective excitation of $PdPc(OBu)_8$ at 720 nm (Figure S16). The triplet sensitization spectra of EH-Fla and TISP-Fla are consistent with that observed in the fsTA spectra at 4 ns.

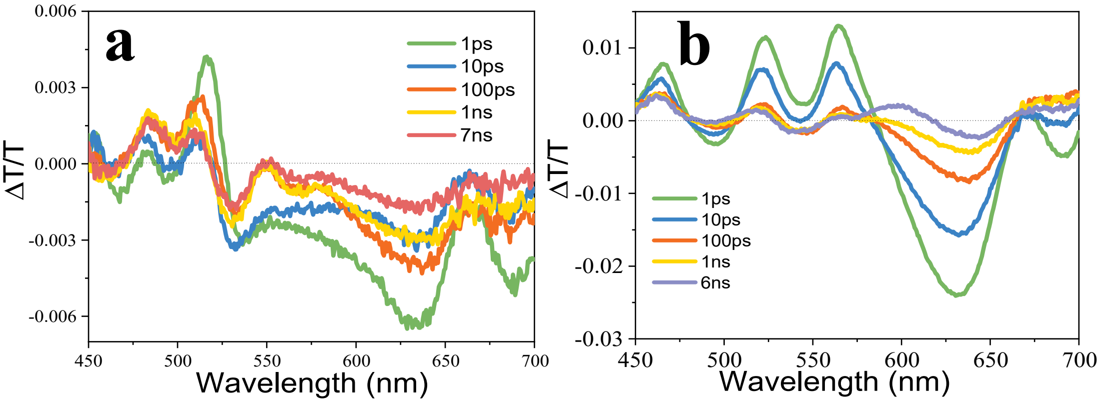

Figure S16. Fs-TA spectra of EH-Fla (a) and TIPS-Fla (b) film doped $PdPc(OBu)_8$ excited at 720 nm.

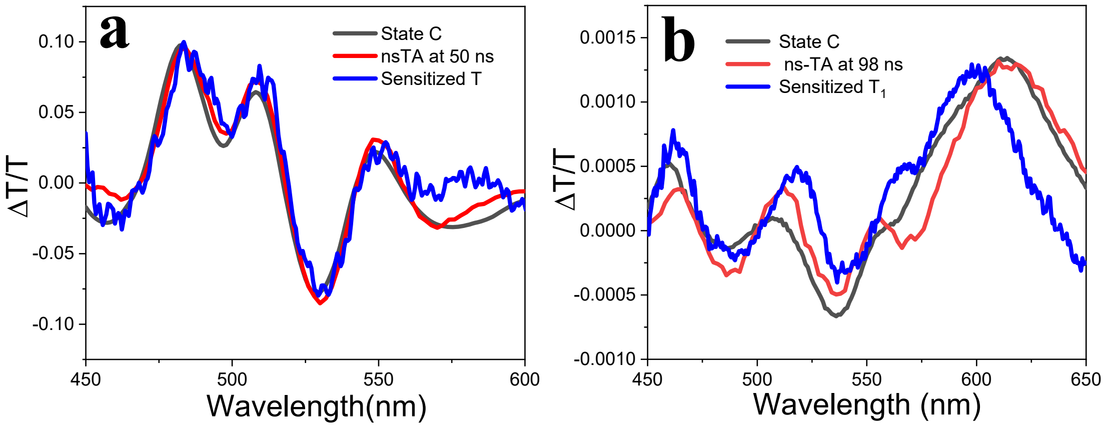

Figure S17. Comparison of the triplet spectra obtained in ns-TA, the triplet spectra obtained from sensitization, state C of EH-Fla (a) and state B of TIPS-Fla (b). The similar line shape suggests that these two species are triplet excitons.

The state C of EH-Fla and state B TIPS-Fla are assigned as triplet pair based on the following reasons. i) The kinetics involving TT→T+T is usually a bi-exponential decay corresponding to triplet pair decay and free triplet decay. But kinetics at 530 nm (EH-Fla) and 542 nm (TIPS-Fla) both show good single-exponential decay (Figure S14). ii) The evolution of the triplet pair to free triplets is strongly temperature-dependent in endothermic singlet fission. From our data, the kinetic curves (Figure S13) at different temperatures are not significantly different, indicating that the kinetic process at the given time scales is temperature-independent. The result indicates that there is no evolution of triplet pairs to free triplet states in the dynamic process in EH-Fla and TIPS-Fla.

In the TIPS-Fla film, the spectra are matched reasonable well between 450 and 650 nm (Figure S17b). We note that, in the sensitization experiments of TIPS-Fla, a much higher concentration of $PdPc(OBu)_8$, than that of EH-Fla, is necessary to obtain an acceptable signal-to-noise ratio for the sensitized triplet state, indicating that the triplet-triplet absorption intensity in TIPS-Fla is much weaker. This weak triplet-triplet absorption in TIPS-Fla makes the sensitization more difficult and can be the reason for the observed small spectral differences shown in Figure S17b. Another possible reason for the slight difference can be attributed to the difference in the nature of the triplets in different experiments. It is known that the long-lived species in the sensitization experiments are free triplet; while the state C in fs-TA spectra and long-lived species in ns-TA spectra are triplet pairs.

Thermal effect

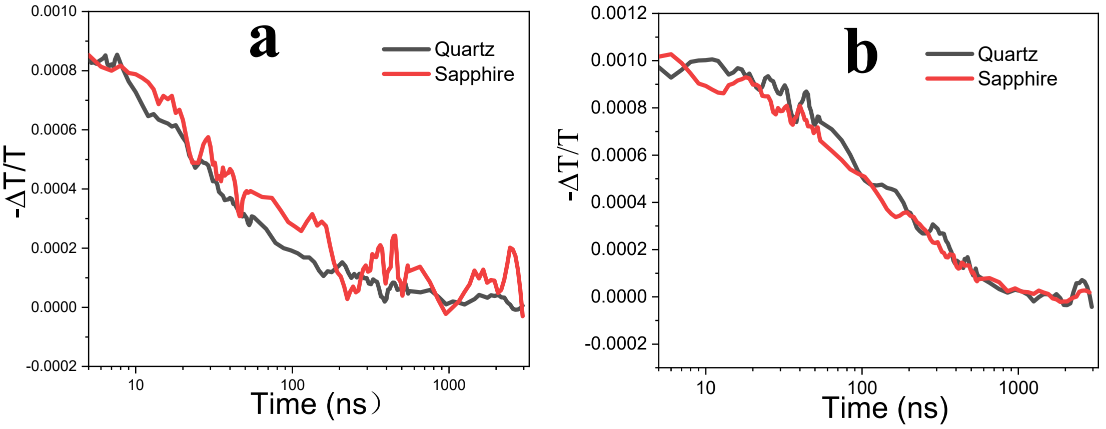

Figure S18. Kinetic curves of EH-Fla (a) and TIPS-Fla (b) on quartz and sapphire substrates from ns-TA spectra.

Triplet yield calculation

The triplet yield is calculated by the method of energy transfer.[2] Here, we converted ΔT/T to ΔOD. First, the extinction coefficient Δε of the flavanthrene triplet excitons can be calculated by a triplet sensitizer with a known triplet molar extinction coefficient. Here, we chose PdPc(OBu)$_8$ as the triplet sensitizer, which can quickly form triplet excitons by ISC. The energy of the triplet excitons is 1.24 eV,[1] which can transfer the triplet energy to the triplet excitons of flavanthrene. The energy transfer yield was determined by comparing the amount of PdPc(OBu)$_8$ that was left over in the film at a given time to determine the relative fraction which has undergone energy transfer. The calculation is as follows:

$$\varepsilon_T = \frac{\Delta OD_{Fla}^{\lambda} \Delta\varepsilon_{PdPc}^{\lambda'}}{\Delta \mathrm{OD}_{PdPc}^{\lambda'} \phi}$$

$\Delta\mathrm{OD}_{\mathrm{PdPc}}^{\lambda'}$ and $\Delta\mathrm{OD}_{\mathrm{Fla}}^{\lambda}$ are the triplet absorption intensities of flavanthrene and PdPc(OBu)$_8$. $\Delta\varepsilon_{\mathrm{PdPc}}^{\lambda'}$ is the molar extinction coefficient of the triplet state of

PdPc(OBu)$_8$ reported in the literature ($\Delta\varepsilon^{\lambda'}_{\mathrm{PdPc}}$=28000M^{-1}cm^{-1}).[3]

Triplet State Extinction Coefficient:

	$\Delta\mathrm{OD}^{\lambda}_{\mathrm{Fla}}$	$\Delta\mathrm{OD}^{675\mathrm{nm}}_{\mathrm{PdPc}}$	ϕ	ε_T(M^{-1}cm^{-1})
EH-Fla	5.34×10^{-4}(530nm)	0.00386	79%	4903
TIPS-Fla	6.26×10^{-4}(540nm)	0.0124	93%	1413

Then we can calculate the concentration of triplet excitons according to the following formula,

$$C_T = \frac{\Delta OD_T}{\varepsilon_T \iota}$$

ι is the thickness of the samples.

	$\Delta\mathrm{OD}_\mathrm{T}$	ι	C_T(M)
EH-Fla	3.17×10^{-5}	220nm	2.94×10^{-4}
TIPS-Fla	3.26×10^{-5}	160nm	1.44×10^{-3}

The excitation density can be calculated according to the following formula.ξ

$$\xi = \frac{E\lambda K(1-10^{-A})}{\iota\alpha}$$

E is the excitation energy, λ is the pump wavelength, K=5.034×10^{-15} J^{-1} nm^{-1}, α = 0.0177cm^{-2}. The concentration of singlet excitons can be calculated. The triplet yield was calculated by the ratio of triplet excitons and singlet excitons concentration.

	E(J)	λ(nm)	α(cm^{-2})	A	ξ	C_S(M)	Φ_T
EH-Fla	2×10^{-7}	400	0.0177	0.34	5.61×10^{17}	9.32×10^{-4}	32%
TIPS-Fla	2×10^{-7}	400	0.0177	0.21	5.45×10^{17}	9.05×10^{-4}	159%

Quantum Chemical calculation

All calculations were performed with the Amsterdam Density Functional (ADF) package.[4] The calculation details were described by Bae et al.[5] Electronic couplings were calculated using density functional theory (DFT) method. The triple ζ with two polarization functions (TZ2P) basis set and the B3LYP exchange-correlation functional[6, 7] were employed. The effective coupling between orbitals i and f, V_{if}, was calculated the using the fragment orbital approach implemented in the ADF package:[8]

$$V_{if} = \frac{J_{if} - \frac{1}{2}S_{if}(e_i + e_f)}{1 - S_{if}^2}$$

Where J_{if} is the Fock matrix element between a pair of monomers, S_{if} is the overlap integral; e_i and e_f are the Fock matrix elements within a monomer.

Table S1. Calculated effective couplings between HOMO and LUMO.

	V_{HH}/ meV	V_{LL}/meV	V_{LH}/meV	V_{HL}/meV
EH-Fla	64.8	123.65	27.42	-27.4
TIPS-Fla	100.02	-159.75	45.17	-33.12

Singlet and triplet excitation energies, E (S_1) and E (T) were calculated using the time-dependent density functional theory (TDDFT). E (TT) was acquired by doubling E (T). The CT state energy, E (CT), was calculated using a Weller-like equation:[9, 10]

$$E\,(CT) = IP + EA + E_{elec} + E_{ind}$$

Here, IP and EA are ionization energy and electron affinity of monomer, respectively. Whereas E_{ind} is the induction energies and E_{elec} is the electrostatic energies. E_{ind} and E_{elec} were calculated using the fully classical Direct Reaction Field (DRF) Force Field method.[11, 12] Mulliken atomic charges were used for both neutral and charged dimers in DRF calculations.

In order to reduce the computational cost, we simplified the molecular models in the calculations. We used OC_2H_5 groups and $Si(CH_3)_3$ groups instead of $OCH_2CH(C_2H_5)C_4H_9$ groups in EH-Fla and $Si(C_3H_7)_3$ groups in TIPS-Fla, respectively. The monomer geometries of EH-Fla and TIPS-Fla were optimized and then placed in their dimer arrangement as determined by their crystal structures.

Table S2. Calculated ionization energy (IP), electron affinity (EA), induction (E_{ind}) and electrostatic (E_{elec}) energies.

	IP/eV	EA/eV	E_{elec}/eV	E_{ind}/eV
EH-Fla	6.39	1.55	-2.01	-0.27
TIPS-Fla	6.40	2.06	-1.97	-0.18

The relative orientation of transition dipole moments (θ) is the angle between transition dipole moments (μ) and displacement vector (R) connecting the molecular mass centres. The transition dipole moments are calculated by TD-DFT. We have calculated the θ values of EH-Fla and TIPS-Fla based on their crystal structures.

Table S2. Calculated transition dipole moments (μ), displacement vector (R) connecting the molecular mass centers and θ.

	μ (atomic unit)	R (Å)	θ
EH-Fla	(-2.1032, 2.6822, 1.1166)	(0, 5.245, 0)	42°
TIPS-Fla	(1.7183, 1.6787, 3.8425)	(0, 3.934, 0)	68°

Assuming that the charge transfer state and the local Frenkel exciton state are well separated (perturbation limit), the CT coupling can be calculated by the following formula,[13]

$$J_{CT} = -2\frac{V_{LL}V_{HH}}{E_{CT} - S_1}$$

Crystal data

Table S4. Crystal data and structure refinement for EH-Fla.

Formula weight	634.83	
Temperature	150.0 K	
Wavelength	1.54178 Å	
Crystal system	Monoclinic	
Space group	P 1 21/c 1	
	a = 17.3779(9) Å	α= 90°.
Unit cell dimensions	b = 5.2454(3) Å	β= 108.694(3)°
	c = 19.4069(10) Å	γ= 90°
Volume	1675.69(16) $Å^3$	
Z	2	
Density (calculated)	1.258 Mg/m^3	
Absorption coefficient	0.590 mm^{-1}	
F(000)	680	
Theta range for data collection	4.811 to 72.122°.	
Index ranges	-21<=h<=21, -6<=k<=6, -23<=l<=22	
Reflections collected	16415	
Independent reflections	3233 [R(int) = 0.0509]	
Completeness to theta = 67.679°	97.7 %	
Absorption correction	Semi-empirical from equivalents	
Max. and min. transmission	0.0872 and 0.0100	

3. References

1 B. D. Rihter, M. E. Kenney, W. E. Ford and M. A. J. Rodgers, *Journal of the American Chemical*

Society, 1990, **112**, 8064-8070.

2 B. J. Walker, A. J. Musser, D. Beljonne and R. H. Friend, *Nat Chem*, 2013, **5**, 1019-1024.

3 P. E. Hartnett, E. A. Margulies, C. M. Mauck, S. A. Miller, Y. Wu, Y. L. Wu, T. J. Marks and M. R. Wasielewski, *J. Phys. Chem. B*, 2016, **120**, 1357-1366.

4 G. te Velde, F. M. Bickelhaupt, E. J. Baerends, C. Fonseca Guerra, S. J. A. van Gisbergen, J. G. Snijders and T. Ziegler, *J. Comput. Chem.*, 2001, **22**, 931-967.

5 Y. J. Bae, G. Kang, C. D. Malliakas, J. N. Nelson, J. Zhou, R. M. Young, Y. L. Wu, R. P. Van Duyne, G. C. Schatz and M. R. Wasielewski, *J. Am. Chem. Soc.*, 2018, **140**, 15140-15144.

6

7 P. J. Stephens, F. J. Devlin, C. F. Chabalowski and M. J. Frisch, *The Journal of Physical Chemistry*, 1994, **98**, 11623-11627.

8 N. Renaud, P. A. Sherratt and M. A. Ratner, *J Phys Chem Lett*, 2013, **4**, 1065-1069.

9

10 H. Oevering, M. N. Paddon-Row, M. Heppener, A. M. Oliver, E. Cotsaris, J. W. Verhoeven and N. S. Hush, *Journal of the American Chemical Society*, 1987, **109**, 3258-3269.

11 M. Swart and P. T. van Duijnen, *Molecular Simulation*, 2006, **32**, 471-484.

12 F. Mirjani, N. Renaud, N. Gorczak and F. C. Grozema, *Journal of Physical Chemistry C*, 2014, **118**, 14192-14199.

13 C. Kaufmann, D. Bialas, M. Stolte and F. Wurthner, *J. Am. Chem. Soc.*, 2018, **140**, 9986-9995.